Molecularly Ordered Inorganic Frameworks in Layered Silicate Surfactant Mesophases

Sean C. Christiansen,[†] Dongyuan Zhao,[‡,§] Michael T. Janicke,[†,⊥] Christopher C. Landry,[‡,||] Galen D. Stucky,[‡] and Bradley F. Chmelka*[,†]

Contribution from the Department of Chemical Engineering, Departments of Chemistry and Materials, University of California, Santa Barbara, California 93106

Received December 20, 2000

Abstract: Self-assembled lamellar silica−surfactant mesophase composites have been prepared with crystal-like ordering in the silica frameworks using a variety of cationic surfactant species under hydrothermal conditions. These materials represent the first mesoscopically ordered composites that have been directly synthesized with structure-directing surfactants yielding highly ordered inorganic frameworks. One-dimensional solid-state ^{29}Si NMR spectra, X-ray diffraction patterns, and infrared spectra show the progression of molecular organization in the self-assembled mesophases from structures with initially amorphous silica networks into sheets with very high degrees of molecular order. The silicate sheets appear to be two-dimensional crystals, whose structures and rates of formation depend strongly on the charge density of the cationic surfactant headgroups. Two-dimensional solid-state heteronuclear and homonuclear NMR measurements show the molecular proximities of the silica framework sites to the structure-directing surfactant molecules and establish local Si−O−Si bonding connectivities in these materials.

Introduction

Mesoporous solids with sharply defined and adjustable pore sizes over the range 1.5−10.0 nm are attractive candidates for catalytic and adsorption applications involving relatively large molecules.[1−4] Such materials have been prepared using cationic surfactant species to produce mesoscopically ordered lamellar (MCM-50), hexagonal (MCM-41), or cubic (MCM-48) structures in approximately micrometer-sized domains. However, until now, such long-range periodic mesostructures have not been accompanied by evidence of the short-range molecular ordering typical of crystalline solids, such as zeolites. For example, the high degree of long-range hexagonal mesoscopic organization and uniformity of siliceous MCM-41 materials is in marked contrast to the short-range disorder of their amorphous silicate walls. X-ray diffraction and ^{29}Si magic-angle spinning (MAS) NMR studies have repeatedly shown that the inorganic oxide frameworks in M41S materials are amorphous both before and after calcination treatments. The desirability of producing molecularly ordered inorganic frameworks lies in the potential for improved adsorption, catalytic, mechanical, and thermal properties of these materials, in addition to providing enhanced resolution for studying interactions at specific inorganic framework sites. Such molecular-level information is crucial for understanding and controlling the placement of other atoms in the framework, which have led to MCM-type materials with diverse macroscopic reaction properties.

Cooperative self-assembly mechanisms and the resultant morphologies of silicate−surfactant mesophases have been examined and are well understood at ambient temperatures in highly alkaline (pH > 12) solutions.[5] Under these conditions, silicate anion species are stable in solution, allowing the process of mesophase self-assembly to be uncoupled from the kinetics of silicate polymerization. As a consequence, it has been possible to prepare lyotropic silicate−surfactant liquid crystals under conditions of thermodynamic equilibrium, which has permitted detailed study of the molecular origins of their phase behaviors.[5] MCM-type structures can be subsequently produced by the polymerization of the oligomeric silicate anions into highly cross-linked networks by reducing the pH or increasing the temperature of the mesophase mixture.

Inter-aggregate interactions among the organic and inorganic moieties play especially significant roles in the formation and structure of inorganic/surfactant mesophases. As a result, considerable effort has been placed on altering the solution conditions and properties of the inorganic−organic interface to modify accordingly the mesophase structure or composition.[4,6] The headgroup moiety of the surfactant is particularly important, because of its position at the hydrophobic−hydrophilic interface, where it interacts directly with the solution environment and, crucially, the inorganic precursor species and subsequent network. Related examples exist in zeolite syntheses, where the

* To whom correspondence should be addressed.
† Department of Chemical Engineering.
‡ Departments of Chemistry and Materials.
§ Present address: Department of Chemistry, Fudan University, Shanghai, 20043, P.R. China.
⊥ Present address: Los Alamos National Laboratory, MS J514/TA-48, Los Alamos NM 87545.
|| Present address: Department of Chemistry, University of Vermont, Burlington, VT 05405.

(1) Beck, J. S.; Vartuli, J. C.; Roth, W. J.; Leonowicz, M. E.; Kresge, C. T.; Schmitt, K. D.; Chu, C. T.-W.; Olson, D. H.; Sheppard, E. W.; McCullen, S. B.; Higgins, J. B.; Schlenker, J. L. *J. Am. Chem. Soc.* **1992**, *114*, 10834−10843.
(2) Kresge, C. T.; Leonowicz, M. E.; Roth, W. J.; Vartuli, J. C.; Beck, J. S. *Nature* **1992**, *359*, 710−712.
(3) Inagaki, S.; Fukushima, Y.; Kuroda, K. *J. Chem. Soc., Chem. Commun.* **1993**, 680.
(4) Huo, Q.; Margolese, D. I.; Ciesla, U.; Demuth, D. G.; Feng, P.; Gier, T. E.; Sieger, P.; Firouzi, A.; Chmelka, B. F.; Schüth, F.; Stucky, G. D. *Chem. Mater.* **1994**, *6*, 1176−1191.
(5) Firouzi, A.; Atef, F.; Oertli, A. G.; Stucky, G. D.; Chmelka, B. F. *J. Am. Chem. Soc.* **1997**, *119*, 3596−3610.
(6) Huo, Q.; Margolese, D. I.; Stucky, G. D. *Chem. Mater.* **1996**, *8*, 1147−1160.

10.1021/ja004310t CCC: $20.00
Published on Web 04/21/2001

use of specific molecular templates (e.g., $(CH_3CH_2)_3N$, $(CH_3)_3N$, $(CH_3)_4N^+$) significantly affects the final architectures of crystalline composites formed under hydrothermal conditions (>100 °C). In an analogous fashion, modifying the surfactant headgroup species used in hydrothermal mesophase syntheses is expected to influence the final molecular structures of the resultant inorganic networks.

Until now, however, the influence of the headgroup of the surfactant species on local ordering of inorganic oxide−mesophase frameworks has not been observed. This has been due, in part, to the difficulty of using elevated temperatures (>140 °C) in surfactant-based inorganic−organic mesophase syntheses. Such conditions can lead to a degradation of the surfactant species, triggering a collapse of the organized mesostructure or the formation of crystalline zeolites.[7−10] The use of lower non-hydrothermal temperatures (<100 °C) allows well-ordered mesostructured products to form, although amorphous inorganic frameworks result, making it difficult to examine the role the headgroup plays in affecting the inorganic order. Such disordered frameworks have been characteristic of all such inorganic oxide−surfactant mesophases observed to date.

Efforts to produce hybrid M41S−zeolite composites have employed hydrothermal synthesis conditions aimed at producing mesoporous solids with crystalline inorganic walls. One such method has used surfactants to produce M41S materials in concert with small amines to nucleate zeolite crystallites in the inorganic walls.[11,12] However, resulting bulk materials are often composed of a segregated mixture of both MCM-41 materials and zeolite crystallites. Similar challenges have also been confronted in postsynthesis treatments of MCM-41 materials with small amines.[13] Thus, the preparation of inorganic−organic mesophase solids with crystalline ordering in the inorganic framework has proven elusive and difficult.

Here, we describe syntheses of self-assembled silica−surfactant mesophase solids (created using a single organic template) that for the first time possess crystal-like molecular ordering in their inorganic frameworks. The molecular structures of the highly ordered frameworks in the lamellar composites are strongly influenced by the surfactant headgroup moieties, whose charge density distributions appear to be a key variable. In addition, the structure-directing function is provided by different components at different stages of the synthesis, initially by self-assembly of the surfactant species and subsequently by two-dimensional crystallization of the inorganic framework. These processes are elucidated through a combination of solid-state NMR, X-ray diffraction, and infrared spectroscopy measurements made on lamellar silica−surfactant composites as mesophase order and subsequent two-dimensional crystallization develop.

Experimental Section

Surfactant Syntheses. The cationic surfactants, cetyltrimethylammonium bromide ($C_{16}NMe_3Br$) and cetyldimethylethylammonium bromide ($C_{16}NMe_2EtBr$), were purchased from Aldrich and required no further preparation. The remaining surfactants, $C_{16}NMeEt_2Br$, $C_{16}NEt_3Br$, and $C_{16}NPr_3Br$, were synthesized from cetyl bromide, $C_{16}Br$ (Aldrich), and an excess of the appropriate alkylamine (i.e., $NMeEt_2$, NEt_3, and NPr_3). The reactants were refluxed for 3−5 days in an ethanolic solution and recrystallized from ethanol/ethyl acetate (3×).[6]

Mesophase Syntheses. Tetramethylammonium hydroxide (TMAOH, 25 wt % in H_2O), hydrobromic acid (HBr), methanol (CH_3OH), and tetramethyl orthosilicate (TMOS) were used as received from Aldrich. Lamellar silica−surfactant composites were prepared at room temperature using the following molar compositions: 1.0 SiO_2: 0.7 surfactant: 0.7 TMAOH: 113.4 H_2O: 9.9 CH_3OH. A typical synthesis procedure involved dissolving an appropriate amount of surfactant in water, after which TMAOH and CH_3OH were added and the solution stirred for 30 min. TMOS was then added and the solution stirred for another 30 min, after which time the pH was lowered to 11.5 with concentrated HBr. After 2 h of stirring, each mixture was aliquoted into a number of identical Teflon-lined Parr reaction vessels which were sealed and placed in an oven at 135 °C. The reaction vessels were individually removed from the oven after specified intervals of time and then allowed to cool to room temperature. The mesophase precipitates were subsequently washed with deionized water to remove any excess surfactant and solvents.

Characterization. X-ray powder diffraction (XRD) data were acquired on a Scintag PAD X diffractometer using Cu K_α radiation and a liquid nitrogen cooled germanium solid-state detector. Typically, the data were collected from 1° to 35° (2θ) with a resolution of 0.02° and a count time of 2s at each point.

Infrared (IR) spectra were recorded with a Nicolet 850 IR spectrometer using the standard KBr pellet method. For each experiment, 256 spectra were accumulated with a resolution of 2 cm^{-1}.

Solid-state nuclear magnetic resonance (NMR) experiments were performed at room temperature on a Chemagnetics CMX-180 spectrometer using a widebore superconducting 4.2 T magnet, except for the spectrum in Figure 8 which was recorded on a CMX-500 spectrometer using a widebore superconducting 11.7 T magnet. A double-resonance magic-angle-spinning (MAS) probehead was used with 7.5 mm Pencil rotors. All cross-polarization experiments were performed at the Hartmann−Hahn mismatch condition:[14] $\gamma_H B_{1H} = \gamma_{Si} B_{1Si} + \omega_r$. ^1H and ^{29}Si chemical shifts were referenced to tetramethylsilane (TMS).

Two-dimensional (2D) $^{29}Si\{^1H\}$ HETeronuclear chemical shift CORrelation (HETCOR) NMR experiments[15,16] were acquired under conditions of magic-angle sample spinning at 5−6 kHz, using a 7.0 μs $\pi/2$ ^1H pulse, followed by a 4.0 ms contact time. The HETCOR experiment exploits short-range through-space dipole−dipole interactions to correlate the chemical shifts of different types of nuclei to elucidate molecular structure. The HETCOR pulse sequence is depicted schematically in Figure 1a and has been described elsewhere, as applied to inorganic−organic mesophase materials.[15,17] Because the magnitudes of the $^1H-^{29}Si$ dipole−dipole couplings vary inversely with the cube of the distance separating the spin pair, only correlations between spatially nearby species (∼<1 nm) are observed in HETCOR spectra. Additional reductions of the magnitude of dipole−dipole couplings can be caused by motion between interacting spin pairs, serving to further decrease the distance over which correlations can be observed. The expansion of the HETCOR spectrum into two frequency dimensions provides significantly improved resolution compared to 1D NMR spectra.

Two-dimensional ^{29}Si Incredible Natural Abundance DoublE QUAntum Transfer Experiments (INADEQUATE) were performed under MAS conditions at 6 kHz using a 7-μs ^1H pulse, followed by a 3.0−4.0 ms contact time, and a τ delay of 15.6 ms (corresponding to 1/4J, where J_{Si-Si}=16 Hz). The INADEQUATE NMR experiment exploits homonuclear, through-bond J couplings that are sensitive to the

(7) Borade, R. B.; Clearfield, A. *Zeolites* **1994**, *14*, 458−461.
(8) Chen, X.; Huang, L.; Quanzhi, L. *J. Phys. Chem. B.* **1997**, *101*, 8460−8467.
(9) Sayari, A.; Kruk, M.; Jaroniec, M.; Moudrakovski, I. L. *Adv. Mater.* **1998**, *10*, 1376−1379.
(10) Beck, J. S.; Vartuli, J. C.; Kennedy, G. J.; Kresge, C. T.; Roth, W. J.; Schramm, S. E. *Chem. Mater.* **1994**, *6*, 1816−1821.
(11) Huang, L.; Guo, W.; Deng, P.; Xue, Z.; Li, Q. *J. Phys. Chem. B.* **2000**, *104*, 2817−2823.
(12) Karlsson, A.; Stöcker, M.; Schmidt, R. *Micro. Meso. Mater.* **1999**, *27*, 181−192.
(13) Kloetstra, K. R.; van Bekkum, H.; Jansen, J. C. *Chem. Commun.* **1997**, *23*, 2281−2282.
(14) Stejskal, E. O.; Schaefer, J. *J. Magn. Res.* **1977**, *28*, 105−112.
(15) Janicke, M. T.; Landry, C. C.; Christiansen, S. C.; Kumar, D.; Stucky, G. D.; Chmelka, B. F. *J. Am. Chem. Soc.* **1998**, *120*, 6940−6951.
(16) Vega, A. J. *J. Am. Chem. Soc.* **1988**, *110*, 1049−1054.
(17) Janicke, M. T.; Landry, C. C.; Christiansen, S. C.; Birtalan, S.; Stucky, G. D.; Chmelka, B. F. *Chem. Mater.* **1999**, *11*, 1342−1351.

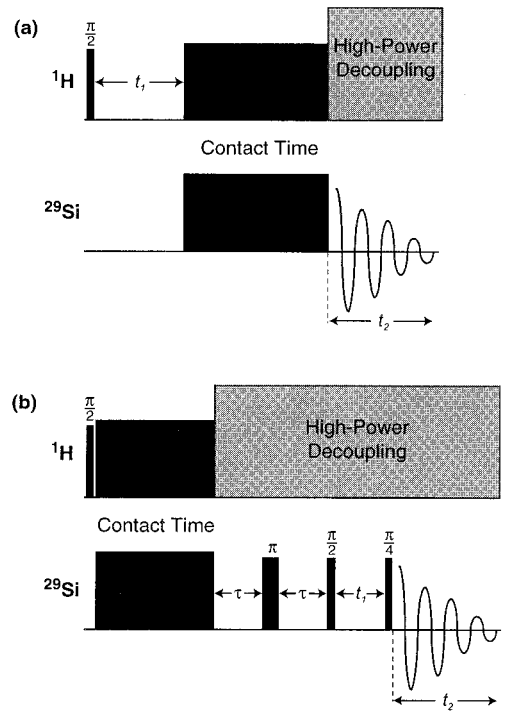

Figure 1. Schematic representations of pulse sequences used for two-dimensional solid-state NMR experiments that (a) correlate ^{29}Si and ^{1}H chemical shifts of nuclei that are dipole−dipole-coupled to each other (the HETCOR experiment) and (b) selectively excite *J*-coupled ^{29}Si−^{29}Si pairs (the so-called INADEQUATE experiment).

hybridization of atomic orbitals and, accordingly, to nearby substituent groups. This method was originally developed to determine the molecular structures of relatively low-molecular weight organic compounds in solution[18] and has also been applied to establish the ^{29}Si−O−^{29}Si site connectivities in solid-state zeolite structures.[19−22]

The 2D INADEQUATE experiment yields enhanced spectral resolution by indirectly detecting double-quantum signals that arise between *J*-coupled species.[18] The double-quantum frequency is the sum of the chemical shifts of two *J*-coupled nuclei with respect to the transmitter frequency, which provides a substantially more sensitive scale for establishing interatomic connectivities compared to *J*-coupling values. The INADEQUATE NMR pulse sequence is depicted schematically in Figure 1b.[23] Initial cross-polarization from ^{1}H to the ^{29}Si spins is used to enhance ^{29}Si signal sensitivity and to take advantage of the short T_1 relaxation times of the ^{1}H species ($T_1 \leq 0.6$ s); by comparison, the T_1 relaxation times of the Q^4 ^{29}Si nuclei are very long ($T_1 \geq 150$ s) in these samples. Following the cross-polarization contact-time, continuous-wave decoupling is applied to the ^{1}H species for the remainder of the experiment to suppress ^{1}H spin diffusion and improve ^{29}Si spectral resolution during detection. While such decoupling is applied, the ^{29}Si magnetization is manipulated with a series of three pulses separated by two delay periods, τ, and an evolution time, t_1, before being detected. The delay periods τ after the cross-polarization period and after the π pulse are optimized for maximum signal intensity when set equal to $1/4J_{Si-Si}$.[24] This allows the magnetization of ^{29}Si nuclei that are *J*-coupled to other ^{29}Si species to be separated from isolated ^{29}Si nuclei that are not. The $\pi/2$ pulse then forces the magnetization of the *J*-coupled ^{29}Si nuclei into double-quantum coherences, which are subsequently converted into single-quantum coherences by the final $\pi/4$ pulse for detection.[25]

For samples containing ^{29}Si in natural abundance (4.7%), this experiment effectively suppresses the otherwise overwhelming single-quantum coherences from isolated ^{29}Si nuclei, while retaining the double-quantum coherences of *J*-coupled ^{29}Si−O-^{29}Si species, which are over an order of magnitude weaker. Filtering the double-quantum signals is made more difficult by the presence of oxygen atoms that are covalently bound between neighboring silicon atoms. Such bridging oxygen atoms reduce the strength of associated ^{29}Si−^{29}Si *J*-couplings, leading to lower signal intensities from ^{29}Si−^{29}Si spin pairs. While several earlier studies have relied on ^{29}Si enrichment to enhance such signals,[22,26,27] ^{29}Si in natural abundance has been used here. The reader is referred to reviews of the theoretical and experimental aspects of the INADEQUATE experiment, which have been published elsewhere.[24,25,28]

Results and Discussion

The inorganic frameworks of self-assembled silicate−surfactant mesophase composites can organize into molecularly ordered sheets under alkaline, hydrothermal conditions. Such highly ordered frameworks are strongly influenced by the headgroups of the surfactant species, which interact via electrostatic interactions, van der Waals forces, etc.[5] To examine the role(s) of the headgroups in determining framework order, silicate−surfactant composites were synthesized with different cetyltrialkylammonium surfactant species. Specifically, the charge density and charge distribution of the trialkylammonium headgroups were systematically varied by modifying the type and combination of the alkyl moieties present using methyl, ethyl, and propyl groups.

I. Silica−Cetyltrimethylammonium ($C_{16}NMe_3^+$) Composites. Standard M41S-type materials synthesized using $C_{16}NMe_3^+Br^-$ as structure-directing surfactant species have yielded highly mesoscopically ordered final products without significant local order in the inorganic framework.[4,6,29] This surfactant possesses a cationic headgroup with three methyl groups (and the C_{16} alkyl chain) attached to the nitrogen atom, presenting a relatively small headgroup over which the monovalent positive charge is distributed. This results in a relatively large average charge density that is approximately symmetric.

The lamellar silica−$C_{16}NMe_3^+$ system was characterized during the course of hydrothermal synthesis to monitor systematically the changes in its morphology and inorganic framework ordering as a function of time. After 1 day under hydrothermal conditions, X-ray powder diffraction (Figure 2a, 1 day) reveals a product with relatively poor lamellar mesostructural order, characterized by a *100* reflection at 3.6 nm and a weak *200* reflection at 1.76 nm. The local molecular organization of the silica framework in this material is shown in the ^{29}Si CP/MAS NMR spectrum (Figure 2b, 1 day) to be amorphous, as characterized by three inhomogeneously broadened resonances centered at −90, −100, and −109 ppm, which are typical of M41S and other siliceous mesophase compos-

(18) Bax, A.; Freeman, R.; Frenkiel, T. A.; Levitt, M. H. *J. Magn. Res.* **1981**, *43*, 478−483.
(19) Morris, R. E.; Weigel, S. J.; Henson, N. J.; Bull, L. M.; Janicke, M. T.; Chmelka, B. F.; Cheetham, A. K. *J. Am. Chem. Soc.* **1994**, *26*, 11849−11855.
(20) Fyfe, C. A.; Feng, Y.; Gies, H.; Grondey, H.; Kokotailo, G. T. *J. Am. Chem. Soc.* **1990**, *112*, 3264−3270.
(21) Fyfe, C. A.; Grondey, H.; Feng, Y.; Kokotailo, G. T. *Chem. Phys. Lett.* **1990**, *173*, 211−215.
(22) Fyfe, C. A.; Gies, H.; Feng, Y.; Grondey, H. *Zeolites* **1990**, *10*, 278−282.
(23) Early, T. A.; John, B. K.; Johnson, L. F. *J. Magn. Res.* **1987**, *75*, 134−138.
(24) Bax, A.; Freeman, R. *J. Magn. Res.* **1980**, *41*, 507−511.
(25) Mareci, T. H.; Freeman, R. *J. Magn. Res.* **1982**, *48*, 158−163.
(26) Fyfe, C. A.; Gies, H.; Feng, Y. *J. Am. Chem. Soc.* **1989**, *111*, 7702−7707.
(27) Fyfe, C. A.; Gies, H.; Feng, Y. *J. Chem. Soc., Chem. Commun.* **1989**, *17*, 1240−1242.
(28) Buddrus, J.; Bauer, H. *Angew. Chem., Int. Ed. Engl.* **1987**, *26*, 625−642.
(29) Vartuli, J. C.; Schmitt, K. D.; Kresge, C. T.; Roth, W. J.; Leonowicz, M. E.; McCullen, S. B.; Hellring, S. D.; Beck, J. S.; Schlenker, J. L.; Olson, D. H.; Sheppard, E. W. *Chem. Mater.* **1994**, *6*, 2317−2326.

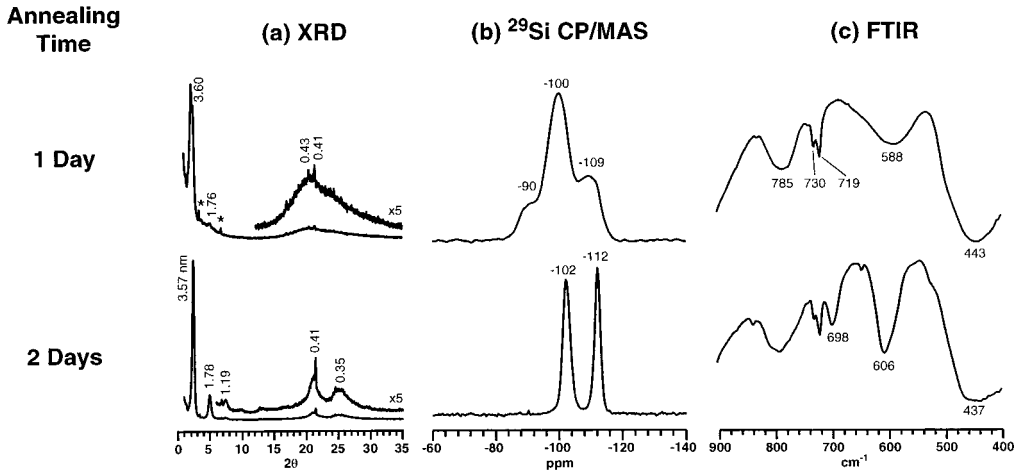

Figure 2. A series of (a) X-ray powder diffraction patterns, (b) ^{29}Si CP/MAS NMR spectra, and (c) FTIR spectra showing progressive mesoscopic and framework ordering in silica−surfactant mesophases synthesized using $C_{16}NMe_3Br$ as the structure-directing species. (* denotes reflection from $C_{16}NMe_3^+$)

ites.[4,6,29,30] These ^{29}Si CP/MAS signals arise from Q^2, Q^3, and Q^4 ^{29}Si species, respectively, where the superscript denotes the number of silicon atoms that are covalently bonded to a central ^{29}Si atom through bridging oxygen atoms.[31] The broad (e.g., Q^3: ∼9 ppm fwhm) overlapping resonances are attributed to a distribution of Si−O−Si bond angles or bond lengths and typifies locally disordered environments in the silica framework.[31] The FTIR spectrum for this material (Figure 2c, 1 day) is displayed over the range 400−900 cm^{-1}, which is dominated by broad absorption bands from the amorphous silica matrix. Bands are observed at 443 and 785 cm^{-1} from the symmetric stretching and bending vibrations of Si−O moieties, along with bands at 719 and 730 cm^{-1} arising from the surfactant species. Inorganic framework vibrations in mesophase composites are, in general, not well understood with respect to specific silica framework structures. However, for zeolites and mineral silicates, IR bands in the region 550−720 cm^{-1} have been attributed to different silicate ring structures.[32−34] While assignment of the broad asymmetrical band at 588 cm^{-1} is still under investigation, bands associated with silica ring structures have not been definitively observed. These results are consistent with the broad ^{29}Si line widths observed in the ^{29}Si MAS NMR spectrum of Figure 2b, indicating a heterogeneous distribution of Si−O−Si bond angles and bond lengths.

For longer hydrothermal treatments under otherwise identical conditions, however, substantial ordering occurs in the silica−$C_{16}NMe_3^+$ composite over both mesoscopic and molecular length scales. For example, after 2 days of hydrothermal synthesis at 135 °C, the silica−$C_{16}NMe_3^+$ product has developed a high degree of lamellar mesoscopic ordering, as evident in the X-ray diffraction pattern of Figure 2a, 2 days, which shows distinct low angle *100*, *200*, and *300* reflections at 3.57, 1.78, and 1.19 nm, respectively. In addition, two broad high-angle reflections are observed at 0.41 and 0.35 nm, which reflect molecular ordering of the silicate framework and likely accompanying organization of the strongly interacting surfactant headgroups.[6,35] More importantly, the ^{29}Si MAS spectrum in Figure 2b, 2 days, shows that the silica framework in the silica−$C_{16}NMe_3^+$ composite has a greatly increased degree of molecular organization, as evidenced by the two narrow ^{29}Si resonances at −102 ppm (Q^3: 2 ppm fwhm) and −112 ppm (Q^4: 2 ppm fwhm). Q^2 species that were previously observed in low concentrations in Figure 2b, 1 day, are not detected, pointing to an increased extent of silica polymerization as a consequence of the longer hydrothermal treatment. These results are consistent with earlier studies of hydrothermally prepared M41S materials,[8,29,36] which however did not examine framework ordering. The FTIR spectrum in Figure 2c, 2 days, shows two bands at 606 and 698 cm^{-1}, which were not previously present. These new signals occur at frequencies that are similar to bands that have been assigned to framework vibrations associated with double-four-membered (D4R) and six-membered rings, respectively, in synthetic silicate compounds.[37−39] The presence of D4R species in the framework matrix would be consistent with previous solution-phase ^{29}Si NMR measurements of Firouzi et al. in alkaline lyotropic silicate−$C_{16}NMe_3^+$ liquid crystals.[5] In these unpolymerized silica systems, preferential interactions were shown to occur between the trimethylammonium headgroup moieties of the surfactant and soluble D4R silicate anions. Longer hydrothermal treatment (up to several weeks) of the ordered silica−$C_{16}NMe_3^+$ composite solid yielded XRD, ^{29}Si NMR, and FTIR data that were unchanged from those in Figure 2, 2 days, indicating that the ordered product is structurally stable.

The two ^{29}Si NMR peaks in Figure 2b at −102 ppm and −112 ppm are confirmed to arise from Q^3 and Q^4 moieties, respectively, in the ordered silica−$C_{16}NMe_3^+$ composite, based on the variations of their signal intensities with ^{1}H−^{29}Si cross-polarization contact time. The presence of nearby protons affects the nuclear spin relaxation rates of ^{29}Si moieties via heteronuclear dipole−dipole couplings. Incompletely polymerized Q^3 (and Q^2) silicon sites are anticipated to have charge-balancing surfactant or silanol species nearby, with associated protons that contribute to more rapid relaxation of Q^3 ^{29}Si species compared

(30) Melosh, N. A.; Lipic, P.; Bates, F. S.; Wudl, F.; Stucky, G. D.; Fredrickson, G. H.; Chmelka, B. F. *Macromolecules* **1999**, *32*, 4332−4342.
(31) Engelhardt, G.; Michel, D. *High-Resolution Solid-State NMR of Silicates and Zeolites*; John Wiley & Sons: New York, 1987.
(32) Jacobs, P. A.; Beyer, H. K.; Valyon, J. *Zeolites* **1981**, *1*, 161−168.
(33) Garces, J. M.; Rocke, S. C.; Crowder, C. E.; Hasha, D. L. *Clays Clay Miner.* **1988**, *36*, 409−418.
(34) Jansen, J. C.; van der Gaag, F. J.; van Bekkum, H. *Zeolites* **1984**, *4*, 369−372.
(35) Tuel, A. *Chem. Mater.* **1999**, *11*, 1865−1875.
(36) Almond, G. G.; Harris, R. K.; Franklin, K. R. *J. Mater. Chem.* **1997**, *7*, 681−687.
(37) Mozgawa, W.; Sitarz, M.; Handke, M. *J. Mol. Struct.* **1999**, *511*−*512*, 251−257.
(38) Sitarz, M.; Mozgawa, W.; Handke, M. *J. Mol. Struct.* **1997**, *404*, 193−197.
(39) Sitarz, M.; Handke, M.; Mozgawa, W. *Spectrochim. Acta, Part A* **1999**, *55*, 2831−2837.

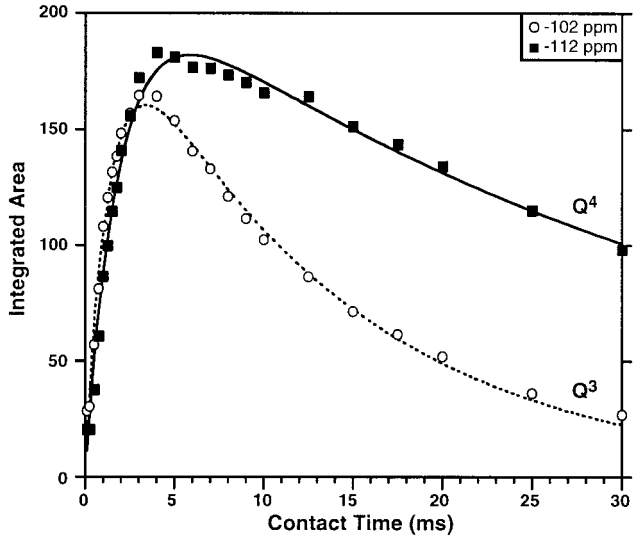

Figure 3. Plots of the integrated ^{29}Si peak areas for the Q^3 (○: −102 ppm) and Q^4 (■: −112 ppm) species measured for various contact times in a series of ^{29}Si CP/MAS experiments performed on the ordered silica−$C_{16}NMe_3^+$ mesophase composite synthesized under hydrothermal conditions at 135 °C for 2 days (see Figure 2b, 2 days). The data have been fit to eq 1 using least-squares analyses, and the results are displayed in Table 1.

to fully polymerized Q^4 ^{29}Si sites. Figure 3 displays plots of the integrated areas of the Q^3 and Q^4 ^{29}Si signals, as functions of the ^{1}H−^{29}Si cross-polarization (CP) contact time. The integrated signal intensities of both ^{29}Si resonances show initial increases for short contact times, according to their respective ^{1}H−^{29}Si cross-relaxation time constants, T_{SiH}. These time constants are characteristic of the approximate strengths of ^{1}H−^{29}Si dipole−dipole couplings and depend on intermolecular distances and dynamics: closer spatial proximities and lower molecular mobilities yield stronger couplings.[40,41] The decreases observed in the integrated signal intensities (Figure 3) at longer contact times arise from proton spin−lattice relaxation in the rotating frame, as described by the characteristic time $T_{1\rho H}$.[42a] Determination of the proton spin−lattice relaxation time constants, $T_{1\rho H}$, was performed using a previously described procedure.[42b] The T_{SiH} relaxation time constants for each ^{29}Si moiety were then determined by fitting the data in Figure 3 to the equation:[43]

$$M(\tau) = M_0\,(\exp(-\tau/T_{1\rho H}) - \exp(-\tau/T_{SiH}))/(1 - T_{SiH}/T_{1\rho H}) \quad (1)$$

using a least-squares analyses, where $M(\tau)$ is the integrated ^{29}Si peak area for the respective signals measured at different contact times τ and M_0 is a normalization parameter determined using least-squares analysis and is proportional to the number of silicon species present. As shown in Table 1, the $T_{1\rho H}$ values for the Q^3 and Q^4 resonances are similar (4.0 and 5.4 ms, respectively) and thus yield limited insight into the molecular differences between these two types of sites. However, the T_{SiH} values are substantially more sensitive to local site structure and dynamics. For example, the Q^3 species (−102 ppm) have a T_{SiH} value of 7.1 ms, which differs markedly from that of the Q^4 species (−112 ppm) for which T_{SiH} = 18.0 ms. This difference in cross-relaxation times is accounted for by the stronger ^{29}Si−^{1}H dipole−dipole couplings and thus shorter cross-relaxation time constants associated with the Q^3 ^{29}Si species, as compared to Q^4 moieties. The relative Q^3 and Q^4 cross-relaxation times measured for the ordered silica−$C_{16}NMe_3^+$ composite vary with sample hydration, but agree well with values previously reported for similar silicate moieties.[40,42]

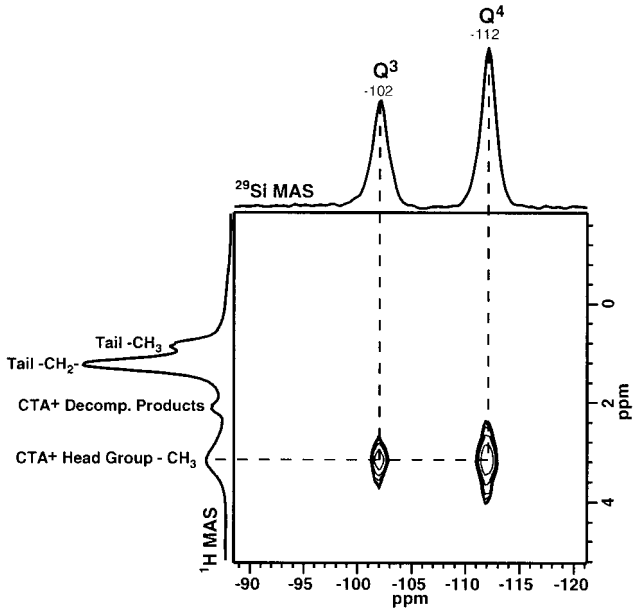

Figure 4. 2D ^{29}Si{^{1}H} HETCOR NMR spectrum acquired for the same ordered silica−$C_{16}NMe_3^+$ mesophase characterized in Figure 2b (2 days) and Figure 3. Separate single-pulse ^{29}Si MAS and ^{1}H MAS spectra accompany the HETCOR contour plot along the horizontal and vertical axes, respectively. The correlations observed in the 2D HETCOR spectrum establish that both Q^3 and Q^4 silicon moieties are interacting strongly with the protons of the surfactant headgroup. 512 acquisitions were recorded for each of the 128 t_1 increments using a 3-s repetition delay.

Table 1. ^{29}Si−^{1}H Cross-relaxation Time Constants (T_{SiH}) and Proton Spin−Lattice Relaxation Time Constants ($T_{1\rho H}$) Determined by Least-Squares Analyses of the Data in Figure 3 Fit to Eq 1 for the Silica−$C_{16}NMe_3^+$ Composite Hydrothermally Synthesized at 135 °C for 2 Days

Si site type	^{29}Si peak (ppm)	T_{SiH} (ms)	$T_{1\rho H}$ (ms)	^{29}Si peak line width (fwhm, ppm)
Q^3	−102	7.1	4.0	2.0
Q^4	−112	18.0	5.4	2.0

On the basis of one-dimensional (1D) NMR methods alone, it is not possible to rule out macroscopic phase separation of the silica and organic species into distinct regions. Such structural questions can be resolved, however, through the use of powerful two-dimensional (2D) NMR techniques, which allow coupled species to be identified and probed. For example, 2D ^{29}Si{^{1}H} heteronuclear correlation (HETCOR) NMR measurements provide detailed insight on interfacial molecular interactions between different silica sites and the proton-containing amphiphilic surfactant species. Figure 4 shows the 2D ^{29}Si{^{1}H} HETCOR contour plot spectrum of the same ordered silica−$C_{16}NMe_3^+$ lamellar mesophase composite studied in Figure 2, 2 days, and Figure 3. Separately acquired single-pulse ^{1}H and ^{29}Si MAS spectra are plotted along the vertical

(40) Zumbulyadis, N.; O'Reilly, J. M. *Macromolecules* **1991**, *24*, 5294−5298.

(41) Leonardelli, S.; Facchini, L.; Fretigny, C.; Tougne, P.; Legrand, A. P. *J. Am. Chem. Soc.* **1992**, *114*, 6412−6418.

(42) (a) Maciel, G. E.; Sindorf, D. W. *J. Am. Chem. Soc.* **1980**, *102*, 7606−7607. (b) Gabrielse, W.; Gaur, H. A.; Feyen, F. C.; Veeman, W. S. *Macromolecules* **1994**, *27*, 5811−5820. (c) Klur, I.; Jacquinot, J.-F.; Brunet, F.; Charpentier, T.; Virlet, J.; Schneider, C.; Tekely, P. *J. Phys. Chem. B* **2000**, *104*, 10162−10167.

(43) Mehring, M. *High-Resolution NMR Spectroscopy in Solids*; Springer-Verlag: New York, 1976.

and horizontal axes, respectively, to aid the interpretation of the 2D data set. In the vertical dimension, the ^{1}H MAS spectrum is composed of resonances arising predominantly from the $C_{16}NMe_3^+$ surfactant species, as indicated. (The weak signal at 2.1 ppm arises from protons associated with a small amount of neutral species resulting from partial decomposition of the surfactant species during the extended hydrothermal synthesis.[44]) The ^{29}Si dimension contains two resonances from the same Q^3 and Q^4 silica moieties previously observed under cross-polarization conditions (Figure 2b). For the 4-ms contact time used, the 2D ^{29}Si{^{1}H} HETCOR spectrum shows strong intensity correlations arising from dipole−dipole couplings between the methyl protons on the $C_{16}NMe_3^+$ surfactant headgroup and both Q^3 and Q^4 ^{29}Si species. Similar ^{29}Si{^{1}H} correlations were observed even for very short contact times down to 100 μs, although with stronger intensity developing first for the Q^3 sites, consistent with their stronger interactions with the surfactant headgroup species. These results establish the close molecular proximities (<1 nm) of the cationic surfactant headgroup to both Q^3 and Q^4 silica species in the ordered inorganic framework.

The ordered lamellar silica−$C_{16}NMe_3^+$ composite appears to share framework structural features in common with a naturally occurring clay mineral, sodium octosilicate. This layered crystalline phyllosilicate has a composition $Na_2O{\cdot}8SiO_2{\cdot}9H_2O$ that yields a ^{29}Si CP/MAS NMR spectrum (not shown here) which is nearly identical to that in Figure 2b, 2 days, with a Q^3 peak at −99.8 ppm (fwhm: 1.2 ppm) and a Q^4 peak at −111.1 ppm (fwhm: 0.3 ppm).[36] The dense three-dimensional mineral structure of crystalline sodium octosilicate, however, also yields a powder X-ray diffraction pattern with numerous high angle reflections, though the crystal structure is still not known.[33] Determining the molecular organization of the inorganic frameworks in layered phyllosilicates is in general a difficult task, even with their local and long-range order, and few phyllosilicate crystal structures have been solved.[36,45] This difficulty is exacerbated in the case of the ordered silica−surfactant composites considered here, because despite the high degree of local framework organization, few high-angle XRD reflections are observed (Figure 2b). Structural characterization challenges are compounded by the absence of large single mesophase domains. For the ordered silica−$C_{16}NMe_3^+$ composite (Figure 2a, 2 days), scanning electron micrographs reveal that the powder sample comprised domains less than 10 μm in size. As a result, little crystallographic information is available to assist with the assignment of framework sites and structural symmetry.

Molecular framework order and the absence of 3D crystallinity in the lamellar silica−$C_{16}NMe_3^+$ composite arise as a result of the disorder and mobility of the alkyl surfactant chains. As individual silicate layers anneal during extended hydrothermal treatment into what are essentially 2D crystalline sheets, the poorly ordered and highly mobile alkyl chain moieties separate and prevent 3D crystalline registry from developing between successive silicate layers.[46] Molecularly ordered silica sheets result, as 2D order nucleates and grows. Within an individual lamellar mesophase domain, the ordered silicate sheets will be uniaxially stacked, possessing transversely isotropic orientations without three-dimensional periodicity (though common symmetry elements should exist with respect to the director normals of the sheets.) For these reasons, the structures of the molecularly ordered frameworks in the composites are difficult to establish.

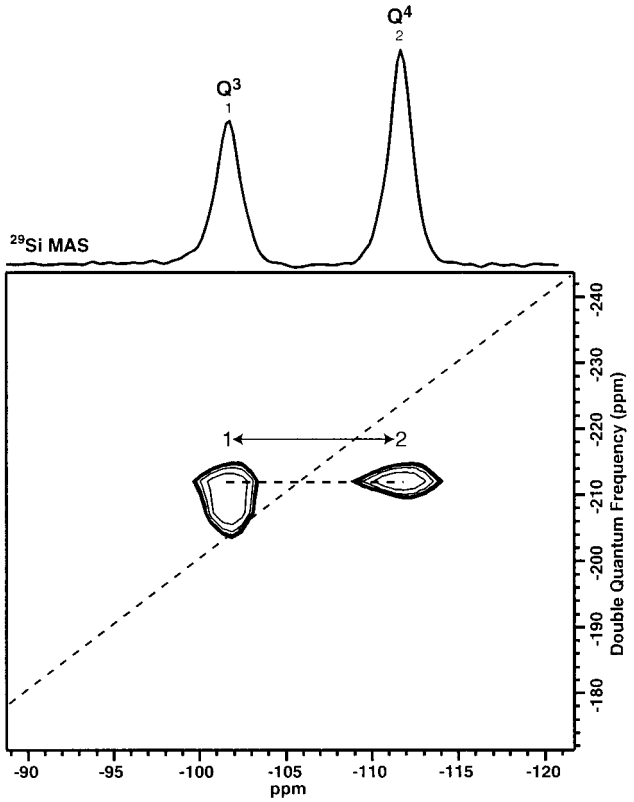

Figure 5. 2D ^{29}Si INADEQUATE NMR spectrum acquired for the same silica−$C_{16}NMe_3^+$ mesophase characterized in Figure 2b (2 days), Figure 3, and Figure 4. A single-pulse ^{29}Si MAS spectrum accompanies the contour plot along the horizontal axis, while the double quantum dimension lies along the vertical axis. The ^{29}Si−^{29}Si correlations observed indicate that tetrahedrally coordinated Q^3 moieties are *J*-coupled to the Q^4 species through a covalently bonded bridging oxygen atom. 8192 acquisitions were recorded for each of the 16 t_1 increments using a 3-s repetition delay.

Nevertheless, detailed additional insight on framework structures with high degrees of molecular order (Figure 2b, 2 days) can be obtained using the 2D solid-state INADEQUATE NMR technique (Figure 1b). The INADEQUATE NMR experiment relies upon homonuclear *J*-couplings between adjacent ^{29}Si sites in a covalently bonded network to establish molecular site connectivities in the siliceous framework structure. For example, Figure 5 presents a contour plot of the 2D ^{29}Si INADEQUATE spectrum for the same ordered silica−$C_{16}NMe_3^+$ composite prepared under hydrothermal conditions at 135 °C for 2 days as examined in Figure 2b, 2 days, and Figures 3 and 4. A quantitative single-pulse ^{29}Si MAS spectrum is shown along the horizontal axis to aid the interpretation of the 2D spectrum. The vertical scale corresponds to the double quantum frequency dimension, in which different *J*-coupled ^{29}Si spin pairs may be resolved. Two covalently bonded ^{29}Si atoms in different sites will share the same double-quantum frequency, though possess

(44) A separate 2D ^{13}C{^{1}H} HETCOR spectrum (not shown here) establishes that the ^{1}H signal at 2.1 ppm arises from the two methyl groups and the α-carbon attached to the uncharged nitrogen atom of *N*,*N*-dimethylhexadecylamine, a product arising from partial thermal decomposition of the $C_{16}NMe_3^+$ surfactant species.[9] The absence of correlated intensity in Figure 4 between the ^{29}Si framework moieties and the protons associated with surfactant degradation products (e.g., *N*,*N*-dimethylhexadecylamine) demonstrates that such nonionic decomposition species are not dipole−dipole-coupled with, and are thus not strongly interacting with, the silicate framework.

(45) Annehed, H.; Fälth, L.; Lincoln, F. J. *Z. Kristallogr.* **1982**, *159*, 203-210.

(46) Burton, A.; Accardi, R. J.; Lobo, R. F.; Falcioni, M.; Deem, M. W. *Chem. Mater.* **2000**, *12*, 2936−2942.

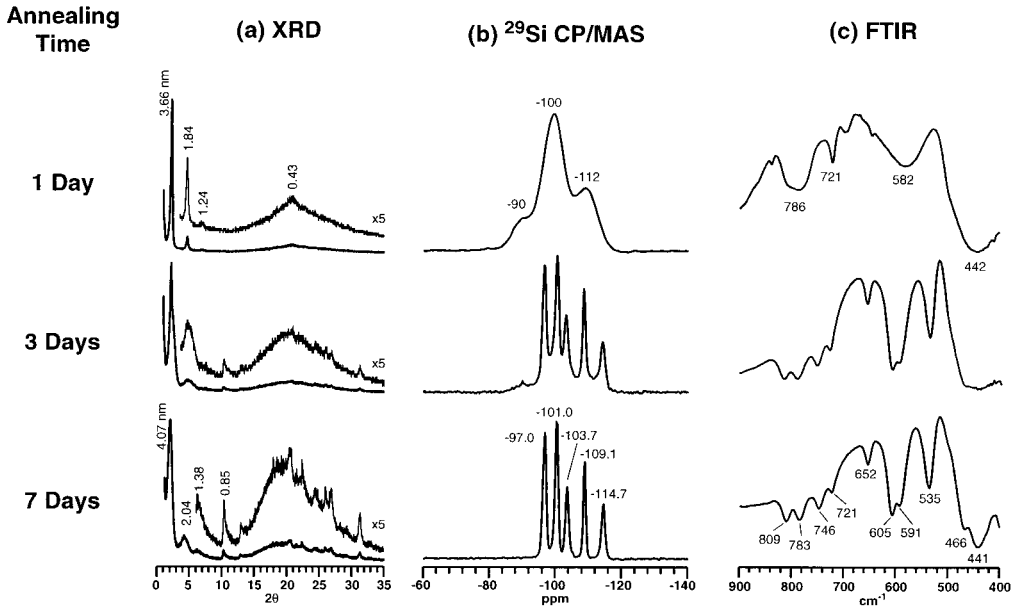

Figure 6. A series of (a) small-angle X-ray powder diffraction patterns, (b) ^{29}Si CP/MAS NMR spectra, and (c) FTIR spectra for silica−surfactant mesophases synthesized using cetyldimethylethylammonium bromide ($C_{16}NMe_2EtBr$) and annealed at 135 °C for different lengths of time.

different isotropic chemical shifts. Inspection of the 2D ^{29}Si INADEQUATE spectrum reveals strong signals that correlate the intensities of the Q^3 and Q^4 resonances. Because of their mutual *J*-coupling of approximately 16 Hz, both the Q^3 and Q^4 ^{29}Si sites possess the same double quantum frequency, from which it can be concluded unambiguously that the Q^3 species are linked through covalent bonds (here, via bridging oxygen atoms) to the Q^4 moieties. As indicated by its designation, ^{29}Si atoms in Q^3 sites are bonded to a terminal oxygen atom (or hydroxyl group). The remaining covalent bonds of such tetrahedrally coordinated Q^3 silicon species are between similar Q^3 silicon sites or to the Q^4 silicon moieties through the bridging oxygen atoms. Similarly, the ^{29}Si INADEQUATE NMR results show that Q^4 sites are covalently bonded to at least one Q^3 site, with the remaining three covalent bonds involving some combination of the Q^4 or Q^3 species. Multiple covalent bonds to similar sites cannot be distinguished on the basis of the INADEQUATE NMR data. These results establish that the ordered silica−$C_{16}NMe_3^+$ composite possesses an interconnected silicate network, with intimately mixed Q^3 and Q^4 species.

II. Silica−Cetyldimethylethylammonium ($C_{16}NMe_2Et^+$) Composites

To examine more generally the role(s) of cationic surfactant headgroups in inducing molecular order in silica frameworks, cetyltrialkylammonium bromide surfactants with different alkylammonium moieties were used to prepare layered silicate−surfactant mesophases under otherwise identical alkaline conditions. For example, instead of the trimethylammonium headgroup moiety present in the ordered silica−$C_{16}NMe_3^+$ composite discussed above, a dimethylethylammonium headgroup was introduced to obtain the cationic surfactant cetyldimethylethylammonium bromide ($C_{16}NMe_2EtBr$). This rather subtle modification to the surfactant species (replacing one of the three methyl groups with an ethyl moiety) yields a slightly larger alkylammonium headgroup with a somewhat reduced and asymmetrically distributed charge density. Using this $C_{16}NMe_2Et^+$ surfactant with the same synthesis procedure described previously, a lamellar silica−$C_{16}NMe_2Et^+$ composite was obtained after 1 day under hydrothermal conditions at 135 °C, as indicated by the XRD pattern shown in Figure 6a, 1 day. The XRD reflections at 3.66, 1.84, and 1.24 nm correspond to the *100*, *200*, and *300* reflections, respectively. The ^{29}Si CP/MAS NMR spectrum of this sample shown in Figure 6b, 1 day, reveals three broad ^{29}Si resonances centered at −90, −100, and −112 ppm that are attributable to Q^2, Q^3, and Q^4 species, respectively. The broad line widths of these ^{29}Si NMR resonances (e.g., Q^3: 9 ppm fwhm) are characteristic of a disordered silica framework, which is similar to that observed for the lamellar silica−$C_{16}NMe_3^+$ mesophase obtained after an identical synthesis time of 1 day (Figure 2). The FTIR spectrum of the silica−$C_{16}NMe_2Et^+$ composite shown in Figure 6c, 1 day, contains a band at 721 cm^{-1} that arises from vibrations due to the surfactant and bands at 442 and 786 cm^{-1} arising from symmetric stretching and bending vibrations of Si−O framework moieties.[32−34] As in the FTIR spectrum of the silica−$C_{16}NMe_3^+$ composite shown in Figure 2c, 1 day, there is an asymmetrical band at 582 cm^{-1} that remains under investigation. Nearly identical XRD, ^{29}Si MAS, and IR results are obtained after 2 days of hydrothermal treatment of silica−$C_{16}NMe_2Et^+$ mesophases under otherwise identical conditions. Thus, hydrothermal syntheses lasting 2 days or less yield lamellar silica−$C_{16}NMe_2Et^+$ mesophase composites, though without any evidence for the formation of locally ordered structures in the inorganic framework.

In contrast, after 3 days of hydrothermal treatment, a lamellar silica−$C_{16}NMe_2Et^+$ composite is obtained with a well-ordered silicate framework. This is evidenced by the emergence of five narrow distinct peaks at −97.0, −101.0, −103.7, −109.1, and −114.7 ppm in the ^{29}Si CP/MAS spectrum of Figure 6b, 3 days. Longer hydrothermal treatment of the composite (to 7 days) leads to improved spectral resolution (Figure 6b, 7 days), with the ^{29}Si peak line widths narrowing to 1 ppm or less. The appearance of the five well-resolved ^{29}Si NMR peaks is accompanied by the presence of both low- and high-angle reflections in the powder X-ray diffraction patterns of Figure 6a, 3 and 7 days. This is indicative of molecular ordering in the silicate sheets and likely accompanying organization of the surfactant headgroups between the inorganic layers. Such a

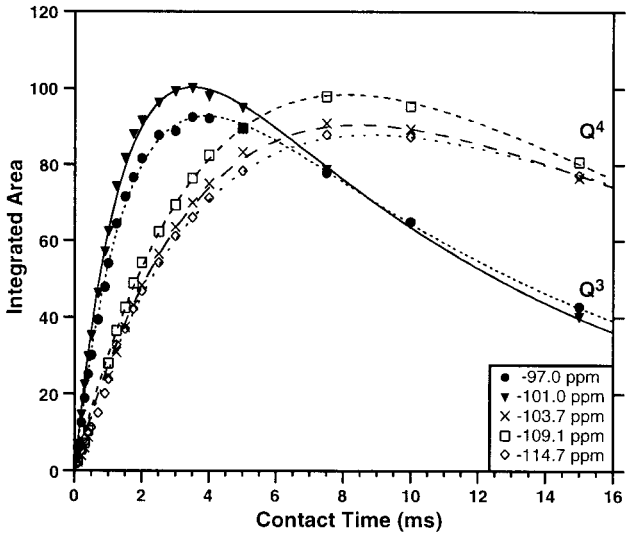

Figure 7. Plots of the integrated ^{29}Si peak areas for Q^3 (●: −97.0 ppm; ▼: −101.0) and Q^4 (×: −103.7 ppm; □: −109.1 ppm; ◇: −114.7 ppm) silica species measured for various contact times in a series of ^{29}Si CPMAS experiments performed on the ordered silica−$C_{16}NMe_2Et^+$ mesophase synthesized under hydrothermal conditions at 135 °C for 7 days (see Figure 6b, 7 days). The data have been fit to eq 1 using least-squares analyses, and the results are displayed in Table 2.

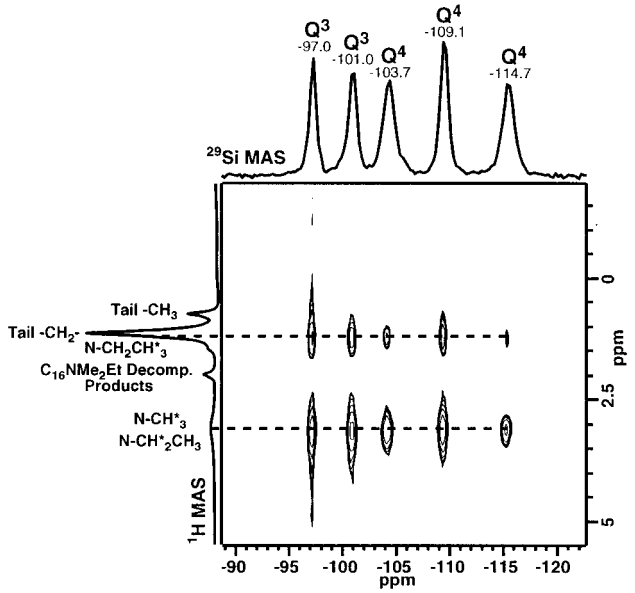

Figure 8. 2D ^{29}Si{^{1}H} HETCOR NMR spectrum acquired for the same ordered silica−$C_{16}NMe_2Et^+$ mesophase characterized in Figure 6b (7 days) and Figure 7. Separate single-pulse ^{29}Si MAS and ^{1}H MAS spectra accompany the HETCOR contour plot along the horizontal and vertical axes, respectively. The correlations observed in the 2D HETCOR spectrum establish that all five silicon moieties are interacting strongly with the methyl and ethyl protons of the surfactant headgroup; 512 acquisitions were recorded at 11.7 T for each of the 108 t_1 increments using a 3-s repetition delay.

structure with five distinct silicon sites is similar to intermediate products obtained during zeolite syntheses, albeit prepared with small molecular templates.[35] FTIR spectra acquired for the ordered lamellar silica−$C_{16}NMe_2Et^+$ composites (Figure 6c, 3 and 7 days) show multiple narrow new bands that are not present in Figure 6c, 1 day, which are attributed to various ordered silicate framework structures. Specifically, the bands at 535, 605, and 652 cm^{-1} arise from vibrations that can be assigned to five-, six-, and four-membered silicate rings, respectively, with the band at 746 cm^{-1} being attributable to vibrations from double-four membered rings.[34,37,38] The bands at 591, 783, and 809 cm^{-1} remain under investigation. These results show that prolonged hydrothermal treatment leads to a molecularly ordered 2D silica network, though with a significantly different local structure from that of the silica−$C_{16}NMe_3^+$ composite discussed above.

To determine the extent of condensation (i.e., Q^3, Q^4) of each of the five ^{29}Si sites in the ordered silica−$C_{16}NMe_2Et^+$ composite, the relaxation time constants, $T_{1\rho H}$ and T_{SiH}, were determined. This is particularly necessary in the present case, because the respective ranges of Q^3 and Q^4 ^{29}Si chemical shifts overlap the positions of several of the peaks observed in Figure 6b. Proton spin−lattice relaxation time constants, $T_{1\rho H}$, were determined as described previously and are shown in Table 2. The results display biexponential relaxation behaviors, which indicate the presence of two types of silicon−proton dipole−dipole couplings.[42c] The T_{SiH} values were subsequently determined from a series of cross-polarization measurements with varying contact times. The resulting integrated intensities for each ^{29}Si peak are plotted in Figure 7 as a function of cross polarization contact time and fit to eq 1. At short contact times, the two downfield peaks (●: −97.0 ppm; ▼: −101.0 ppm) display a more rapid initial increase in intensity than the three upfield peaks peaks (×: −103.7 ppm; □: −109.1 ppm; ◇: −114.7 ppm). As previously discussed, this is characteristic of stronger heteronuclear dipole−dipole couplings between Q^3 ^{29}Si sites and proton species associated with hydroxyl moieties or surfactant headgroups, resulting in shorter cross-polarization and relaxation time constants, T_{SiH} and $T_{1\rho H}$ (Table 2), compared to fully condensed Q^4 ^{29}Si sites. Thus, the ^{29}Si isotropic chemical shifts of the peaks in Figure 6b, 7 days, and their corresponding cross-polarization and relaxation times establish the two downfield peaks to be Q^3 moieties and the three upfield peaks to be fully polymerized Q^4 species.

Table 2. ^{29}Si−^{1}H Cross-relaxation Time Constants (T_{SiH}) and Proton Spin−Lattice Relaxation Time Constants ($T_{1\rho H}$) Determined by Least-squares Analyses of the Data in Figure 7 Fit to Eq 1 for the Silica−$C_{16}NMe_2Et^+$ Composite Hydrothermally Synthesized at 135 °C for 7 Days

Si site type	^{29}Si peak (ppm)	T_{SiH} (ms)	$T_{1\rho H}$ (ms)	^{29}Si peak line width (fwhm, ppm)
Q^3	−97.0	2.4	1.5	1.1
		5.1	12.5	
Q^3	−101.0	3.1	1.3	1.0
		5.0	12.7	
Q^4	−103.7	5.1	1.1	1.0
		13.2	10.9	
Q^4	−109.1	5.5	1.2	0.8
		11.9	12.2	
Q^4	−114.7	2.4	1.5	1.1
		11.5	11.3	

To determine whether the various Q^3 and Q^4 silica species occupy sites in the inorganic framework of the ordered silica−$C_{16}NMe_2Et^+$ mesophase, 2D ^{29}Si{^{1}H} HETCOR data were acquired to probe heteronuclear dipole−dipole couplings between the ^{29}Si moieties and protons of the structure-directing surfactant species. A ^{29}Si{^{1}H} HETCOR spectrum is shown in Figure 8 for the molecularly ordered lamellar composite hydrothermally synthesized at 135 °C for 7 days using $C_{16}NMe_2EtBr$. The accompanying 1D ^{1}H MAS spectrum is composed of resonances arising predominantly from the surfactant, $C_{16}NMe_2Et^+$, and from a small quantity of its thermal decomposition products. Its appearance is similar to the 1D ^{1}H MAS spectrum of Figure 4 for the ordered silica−$C_{16}NMe_3^+$ composite, with the exception that additional contributions from

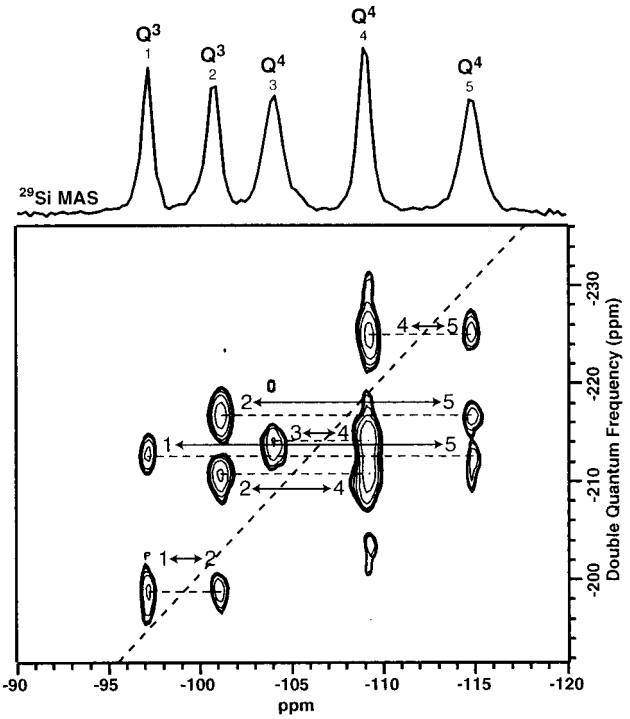

Figure 9. 2D ^{29}Si INADEQUATE NMR spectrum acquired for the same ordered silica$-C_{16}NMe_2Et^+$ mesophase characterized in Figure 6b (7 days), Figure 7, and Figure 8. A single-pulse ^{29}Si MAS spectrum accompanies the contour plot along the horizontal axis, while the double quantum dimension lies along the vertical axis. The atomic connectivities between pairs of silicon atoms can be established from the correlated intensities at identical double-quantum frequencies. 2048 acquisitions were recorded at for each of the 96 t_1 increments using a 2-s repetition delay.

the methylene ($-CH_2$-) and methyl species associated with the ethyl headgroup moiety exist at 1.2 and 3.1 ppm, respectively, although they overlap other signals present. The 1D ^{29}Si MAS spectrum contains the five resonances previously recorded under cross-polarization conditions (Figure 6b, 7 days), although with integrated peak areas that establish 1:1:1:1:1 relative populations. The 2D HETCOR spectrum shows clear chemical shift correlations between all five ^{29}Si sites and the protons associated with the surfactant headgroup. This establishes that the protons attached to the two methyl headgroup moieties ($N-C\mathbf{H}_3$: 3.1 ppm) and the single ethyl headgroup species ($N-C\mathbf{H}_2CH_3$: 3.1 ppm, $N-CH_2C\mathbf{H}_3$: 1.2 ppm) are dipole−dipole coupled to each of the five different ^{29}Si sites. This provides unambiguous evidence that a substantial fraction (if not all) of the five different silica species are molecularly adjacent (<1 nm) to the cationic headgroup of the structure-directing $C_{16}NMe_2Et^+$ surfactant species, consistent with incorporation of the different ^{29}Si sites into the molecularly ordered silica sheet framework.

The 2D INADEQUATE ^{29}Si NMR spectrum in Figure 9 establishes the intra-framework connectivities between covalently linked Q^3 and Q^4 ^{29}Si moieties in the ordered silica$-C_{16}NMe_2Et^+$ product. The contour plot of the 2D ^{29}Si INADEQUATE spectrum shows numerous correlations among the different ^{29}Si species for a delay time τ of 15.6 ms that corresponds to a *J*-coupling constant of 16 Hz.[47] For example, correlated signal intensity in the 2D spectrum is observed between site 2 (Q^3: −101 ppm) and sites 1, 4, and 5. As discussed above (Figure 5), such correlations arise from intramolecular *J*-couplings between covalently connected species. Thus, Q^3 site 2 is shown to have covalent linkages to silicate sites 1, 4, and 5 (each through a bridging oxygen atom). The remaining fourth bond for the tetrahedrally coordinated Q^3 ^{29}Si species 2 is a terminating hydroxyl (or $-O^-$) group. Similarly, $^{29}Si-^{29}Si$ *J*-coupling correlations are measured between site 5 and sites 1, 2, and 4, thus establishing adjacent intra-framework tetrahedral positions for these species in the ordered silica framework. That only three of the four neighboring ^{29}Si species for Q^4 site 5 are accounted for indicates either a second covalent linkage to one of the other three moieties or a covalent linkage to another site like itself, which are not discernible in the INADEQUATE spectrum. This is also the case for Q^4 site 4, which shows correlated intensity with sites 2, 3, and 5; the fourth neighboring site is expected to be a second linkage to one of these species or to another site 4 species. By similar analysis and reasoning, the INADEQUATE NMR spectrum in Figure 9 shows that Q^3 site 1 shares covalent linkages with species 2 and 5 and a terminal hydroxyl (or $-O^-$) group. The fourth unaccounted for bond of tetrahedrally coordinated site 1 will be a second covalent linkage to species 2 or 5 or another site like itself. Finally, Q^4 site 3 in this manner is shown to share the fewest intensity correlations with the other framework sites, manifesting only one linkage to species 4 through a bridging oxygen atom. The remaining three tetrahedral site neighbors of site 3 thus appear to be one or more site 3 or 4 species. These results confirm that the highly ordered framework in the silica$-C_{16}NMe_2Et^+$ composite comprises a densely interconnected network that appears to preclude the possibility that multiple macroscopically distinct phases exist.

Whereas the ordered silica$-C_{16}NMe_3^+$ composite was shown to have an inorganic framework resembling an octosilicate-type structure with two resolvable ^{29}Si species (Figure 2b, 2 days), the ordered silica$-C_{16}NMe_2Et^+$ composite has five distinct ^{29}Si sites, (Figure 6b, 7 days). Moreover, the molecular environments in the framework of the silica$-C_{16}NMe_2Et^+$ material are even more highly ordered, yielding ^{29}Si peak line widths of 0.8−1.1 ppm fwhm, compared to ∼2.0 ppm for the silica$-C_{16}NMe_3^+$ product. Similar molecular ordering has recently been noted by Tuel in intermediates present during syntheses of zeolites in which tetraethylammonium hydroxide was used as a molecular template.[35] In this study, materials with five distinct ^{29}Si MAS resonances were observed with isotropic chemical shifts that are different from those observed here. In addition, the FTIR spectrum for the silica$-C_{16}NMe_2Et^+$ material (Figure 6c, 7 days) indicates the presence of a variety of silicate ring structures that are more numerous than observed in the ordered silica$-C_{16}NMe_3^+$ composite. On the basis of these results, particularly the 2D ^{29}Si INADEQUATE spectrum, the number of different arrangements of the silicate framework is significantly constrained to only five candidate configurations that are consistent with the data. The silicon site connectivities of these structures are provided as Supporting Information, and efforts are currently underway in our laboratory to determine the correct framework configuration.

An added consequence of using $C_{16}NMe_2Et^+$ as the structure-directing surfactant is that the duration of the hydrothermal synthesis required to obtain a composite with an ordered silicate framework increases to 7 days, compared to the 2 days needed when $C_{16}NMe_3^+$ is used. The relative swiftness of the latter can be attributed to the high charge density of the hydrophilic−

(47) A separate 2D ^{29}Si INADEQUATE spectrum (not shown here) was acquired from the same silica$-C_{16}NMe_2Et^+$ composite using a delay period τ of 12.5 ms, corresponding to a *J*-coupling constant of 20 Hz. The resulting spectrum contained correlations similar to those observed in Figure 9, indicating that no stronger correlations in this range of interaction strengths appear to be present.

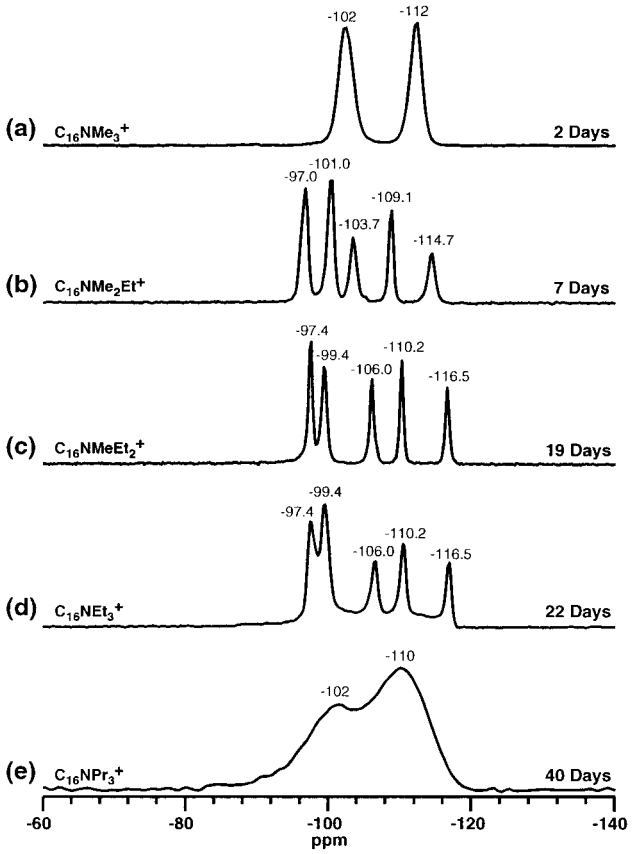

Figure 10. A series of ^{29}Si CP/MAS NMR spectra acquired on lamellar silica−surfactant mesophase composites synthesized using surfactants with different cationic cetyltrialkylammonium headgroups under otherwise identical hydrothermal conditions at 135 °C until molecularly ordered silicate frameworks were obtained. The times required for such ordering to occur depend strongly on the charge densities of the cationic surfactant headgroups, with higher charge densities promoting more rapid formation of ordered frameworks.

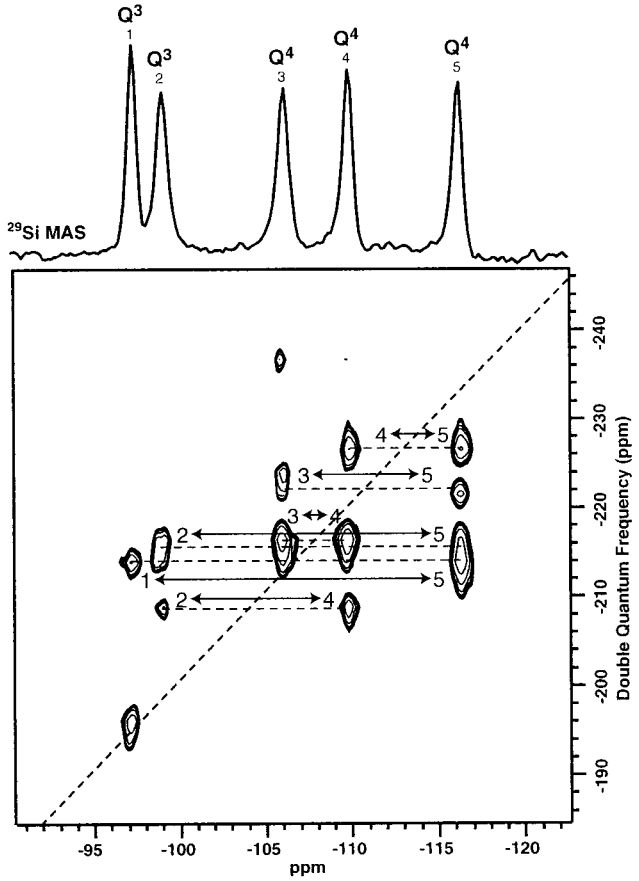

Figure 11. 2D ^{29}Si INADEQUATE NMR spectrum acquired for the same ordered silica−$C_{16}NMeEt_2^+$ mesophase characterized in Figure 10c, 19 days. A single-pulse ^{29}Si MAS spectrum accompanies the contour plot along the horizontal axis, while the double quantum dimension lies along the vertical axis. The correlations observed reveal structural connectivities between framework silicon atoms that correspond to a different framework structure compared to the material synthesized using $C_{16}NMe_2EtBr$ species (Figure 9). 2048 acquisitions were recorded for each of the 114 t_1 increments using a 2-s repetition delay.

NMe_3^+ headgroup. Replacement of one of the methyl moieties on the trialkylammonium headgroup with an ethyl group ($-CH_2CH_3$), results in a lower and asymmetrical charge density distribution. Framework ordering using this surfactant ($C_{16}NMe_2Et^+$) still occurs, but at a significantly slower rate, yielding an entirely different molecularly ordered silicate sheet structure after 7 days. The longer hydrothermal treatment required to achieve a highly ordered composite appears to be due to the lower charge density of the $-NMe_2Et^+$ headgroup and the correspondingly weaker electrostatic interactions at the silicate−surfactant interface. This will be discussed in more detail below.

III. Other Silica−Cetyltrialkylammonium Surfactant Composites

The ^{29}Si MAS NMR spectra of lamellar silica−surfactant composites obtained after extended hydrothermal treatments with different cationic trialkylammonium headgroups are displayed in Figure 10. Figure 10a,b shows the ^{29}Si CP/MAS spectra of the ordered products obtained using $C_{16}NMe_3^+$ and $C_{16}NMe_2Et^+$, respectively, as the structure-directing species, as discussed in detail above. When the trialkylammonium headgroup of the cationic surfactant was modified to include a methyl and two ethyl group moieties, $C_{16}NMeEt_2^+$, a lamellar composite with an amorphous silica framework again resulted after hydrothermal syntheses lasting as long as 9 days, as evidenced by XRD and ^{29}Si MAS NMR results (not shown here). As with the two previous cases, the silica−$C_{16}NMeEt_2^+$ composite similarly transformed into a product with a highly ordered silicate framework. This process began after approximately 10 days under hydrothermal conditions and was completed after 19 days, as evidenced by the ^{29}Si CP/MAS spectrum in Figure 10c, which contains no discernible signal from amorphous silica. This lengthened hydrothermal treatment is consistent with the lower charge density of the surfactant headgroup, which is expected to interact still more weakly with the anionic inorganic framework. The ^{29}Si CP/MAS spectrum of the ordered lamellar silica−$C_{16}NMeEt_2^+$ composite (Figure 10c) shows five narrow (0.8−1.1 ppm fwhm) ^{29}Si peaks at isotropic chemical shifts of −97.4, −99.4, −106.0, −110.2, and −116.5 ppm. These are different from the positions of the five ^{29}Si resonances measured for the silica−$C_{16}NMe_2Et^+$ material, indicating that these materials possess different framework structures with different molecular environments surrounding each ^{29}Si species. This is confirmed by the 2D INADEQUATE ^{29}Si NMR spectrum of the silica−$C_{16}NMeEt_2^+$ composite in Figure 11, which shows very different sets of ^{29}Si−^{29}Si correlations that reveal different silicate site connectivities compared to the ordered silica−$C_{16}NMe_2Et^+$ composite. Specifically, Q^4 site 5 displays correlated intensity with each of the other four species, sites 1, 2, 3, and 4, which result from *J*-couplings through covalent bonds via bridging oxygen atoms. By comparison, the INADEQUATE

spectrum in Figure 9 for the silica−$C_{16}NMe_2Et^+$ composite showed no correlation between sites 5 and 3. Similarly, Figure 9 shows a clear correlation between sites 1 and 2, which is not observed in the 2D INADEQUATE ^{29}Si spectrum of the silica−$C_{16}NMeEt_2$+ composite in Figure 11. In this case, these results constrain the molecular structure of the silicate framework to three possible scenarios, with silicon site connectivities that are tabulated and available as Supporting Information. The possible bonding schemes do not match and are distinct from the candidate structures for the silica−$C_{16}NMe_2Et^+$ composite, affirming the strong structure-directing functions of the surfactant headgroups on the molecular organization of the ordered silicate frameworks.

When three ethyl or three *n*-propyl groups are present, producing even larger cationic trialkylammonium surfactant headgroups, still weaker, although symmetric, charge density distributions result. These surfactants were used to determine whether the degree of headgroup asymmetry plays a significant role in the crystallization of the silicate network. Consistent with the results presented above, silicate−surfactant composites take longer to form molecularly ordered frameworks, as the size of the cationic trialkylammonium headgroups increases and the charge density is reduced. Figure 10d shows the ^{29}Si CP/MAS NMR spectrum from the lamellar silica−$C_{16}NEt_3^+$ composite synthesized under hydrothermal conditions at 135 °C for 22 days. In this spectrum, five ^{29}Si peaks are observed at the identical isotropic shifts measured in the composite prepared using $C_{16}NMeEt_2^+$ (Figure 10c). In addition, a broad ^{29}Si signal is also present in this spectrum, indicating that a small fraction of poorly ordered silica still remains after several weeks of hydrothermal treatment. No molecular order in the framework in fact is observed at all until after 13 days, when the initial appearance of narrow components in the ^{29}Si MAS spectrum is first observed. Attempts to record a 2D ^{29}Si INADEQUATE spectrum for this sample were hampered by the incompletely crystallized silica sheets of this silicate−$C_{16}NEt_3^+$ composite (leading to a distribution of *J*-couplings), so that the molecular connectivities in the inorganic framework could not be determined. The close similarity of the 1D ^{29}Si CP/MAS spectra in Figure 10c,d, however, suggests similar ordered framework structures in the silica−$C_{16}NMeEt_2^+$ and silica−$C_{16}NEt_3^+$ composites. By comparison, cationic cetyltripropylammonium surfactant species yield a lamellar composite, although after 40 days of hydrothermal treatment, no discernible framework order is observed. These results establish that higher surfactant headgroup charge densities lead to more rapid crystallization of layered silicate sheets in lamellar silicate−cetyltrialkylammonium composites under alkaline hydrothermal conditions.

The molecular organization of the inorganic silica in these materials is dependent upon the organic template species used, as well as the temperature employed. Increased synthesis temperatures (>140 °C) resulted in decomposition of the surfactant, leading to subsequent degradation of framework order. In these cases, the remnants of the structure-directing surfactant species exert a weak influence on the inorganic architecture, resulting in materials that are mesoscopically disordered and locally amorphous. These results emphasize the importance of both the hydrothermal synthesis temperature and the charge density of the surfactant species on the structure of the mesoscopically ordered inorganic framework. Such considerations are related to syntheses of crystalline zeolites, where molecular template species are known to influence the molecular structures of the resultant inorganic networks.

Conclusions

Lamellar silicate−cetyltrialkylammonium composites with highly ordered inorganic frameworks were prepared by systematically varying the charge density and symmetry of the hydrophilic surfactant headgroup moieties under otherwise identical hydrothermal alkaline synthesis conditions. All of the resulting materials possessed lamellar mesostructural order with initially amorphous silica frameworks. With extended hydrothermal treatment at 135 °C; however, the disordered frameworks transformed into molecularly ordered silicate sheets in times that depended strongly on the charge-density of the surfactant headgroups, according to the sequence: $-NMe_3^+ < -NMe_2Et^+ < -NMeEt_2^+ < -NEt_3^+ < -NPr_3^+$. Furthermore, 1D and 2D solid-state NMR methods show that different headgroup moieties yield ordered frameworks with generally different 2D crystalline structures. While the silicate−$C_{16}NMe_3^+$ composite has an ordered framework resembling an octosilicate mineral structure, $C_{16}NMe_2Et^+$ and $C_{16}NMeEt_2^+$ surfactant species yielded ordered frameworks with distinct structures that appear to be different from known naturally occurring or synthetic minerals. These results provide new understanding of the molecular factors that promote the crystallization of ordered inorganic frameworks in composite mesophases. Efforts are underway in our laboratory to incorporate such insights into the design and synthesis of mesoporous solids with molecularly ordered frameworks, with the aim of enhancing the catalytic properties of these systems.

Acknowledgment. We thank Dr. D. Kumar, Dr. A. Davidson, and Dr. L. M. Bull for helpful discussions at early stages of these investigations and Dr. F. Babonneau for discussions of the NMR relaxation measurements. We also gratefully acknowledge one of the anonymous reviewers for several helpful comments and suggestions. This work was supported in part by the U.S. Army Research Office under Grant number DAAH04-96-1-0443 (S.C.C., M.T.J., B.F.C.) and by the U.S. National Science Foundation through Grant DMR-9634396 (D.Z., C.C.L., G.D.S.) using central facilities of the NSF-supported UCSB Materials Research Laboratory under award DMR-9632716.

Supporting Information Available: For the ordered silica−$C_{16}NMe_2Et^+$ and the silica−$C_{16}NMeEt_2^+$ frameworks, candidate silicon site connectivities are provided, based on ^{29}Si INADEQUATE NMR results in Figures 9 and 11 (PDF). This material is available free of charge via the Internet at http://pubs.acs.org.

JA004310T